Poissonian twin-beam states and the effect of symmetrical photon subtraction in loss estimations

N. Samantaray,[1,2,*] J. C. F. Matthews,[1] and J. G. Rarity[1]

[1]*Quantum Engineering Technology Labs, H. H. Wills Physics Laboratory and Department of Electrical and Electronic Engineering, University of Bristol, Bristol BS8 1FD, United Kingdom*

[2]*Department of Physics, University of Strathclyde, John Anderson Building, 107 Rottenrow, Glasgow G4 0NG, United Kingdom*

(Received 26 September 2020; revised 17 October 2021; accepted 22 November 2021; published 27 December 2021)

We have devised an experimentally realizable model generating twin-beam states whose individual beam photon statistics are varied from thermal to Poissonian (by temporal mode averaging) keeping the nonclassical mode correlation intact. We have studied the usefulness of these states for loss measurement by considering three different estimators, comparing with the correlated thermal twin-beam states generated from spontaneous parametric down conversion or four-wave mixing. We then incorporated the photon subtraction operation into the model and demonstrated their performance in loss estimations with respect to unsubtracted states at both fixed squeezing and per photon exposure of the absorbing sample. For instance, at fixed squeezing, for two photon subtraction, up to three times advantage is found. An unexpected result in the latter case is that in some operating regimes the photon subtraction scheme can also give up to 20% advantage over the correlated thermal beam result and no advantages are obtained when the statistics of each beam turns to Poissonian. We have also made a comparative study of these estimators for finding the best measurement for loss estimations. We present results for all the values of the model parameters changing the statistics of twin-beam states from thermal to Poissonian.

DOI: 10.1103/PhysRevA.104.063718

I. INTRODUCTION

Absorption based measurement underpins many approaches to spectroscopy and imaging. It finds application in all branches of science from chemistry and biology to physics and material science. However, the best sensitivity in loss estimation reached so far using classical light probes is limited by photon shot noise. In past years, nonclassical resources such as non-Gaussian states (by de-Gaussification of Gaussian states) have shown how to reach the sub-shot-noise (SSN) limit in loss estimations in terms of Fisher information [1]. De-Gaussified single mode squeezed vacuum has been reported for theoretical quantum enhancement in loss estimation [2]. Two basic operations that can lead to non-Gaussian states are photon addition to, or photon subtraction from, Gaussian light states [3,4]. Another important feature of bipartite quantum states to reach the sub-shot-noise limit (SSNL) are nonclassical correlations [5].

It is known that the twin-beam state (TBS) generated by the spontaneous parametric down conversion (SPDC) or four wave mixing (FWM) process has thermal photon statistics in the individual modes, but its perfect photon number nonclassical mode correlation allows surpassing the shot-noise limit (SNL) reaching SSN sensitivity in the realistic scenario of loss estimations [6–12]. More recently, unbiased estimations of optical losses [13] (losses are estimated in an absolute way without precalibration of the apparatus) at the ultimate quantum limit have been reported exploiting the quantum correlations in TBS. In the laboratory context, these correlated beams usually appear Poissonian due to temporal (or spatial) averaging of thermal statistics [14]. Bandwidth and gating time were varied using the pulse pump to show transition from thermal (Gaussian) to Poissonian. In our model we have explored such types of averaging of thermal statistics in details which will be useful for simulating results for realistic quantum metrological applications.

De-Gaussification by symmetrical photon subtraction on both of the modes of TBS has not only been shown to improve the individual mode photon statistics from thermal to sub-Poissonian [15], but it also increases the entanglement between them [16–18]. In the past years, the resulting TBS states after photon subtraction have been theoretically investigated reporting their advantage over TBS for target detection in the presence of noise, the so-called "quantum illumination" [19]. Their advantage over TBS has also been demonstrated in single interferometry with parity measurements [20] and more recently for probing the Planck scale physics [21] and distillation of squeezing [22]. Looking at all these advantages of symmetrical photon subtracted TBS (SPSTBS) over TBS because of their improved photon statistics and nonclassical correlation, we proliferated our interest for using multithermal averaged SPTBS for loss estimations. However, a question on fundamental grounds naturally arises: does photon subtraction have any advantage in noise suppression if the individual mode photon statistics of TBS becomes Poissonian (due to averaging of thermal statistics). Keeping this motivation in mind, we have devised a theoretical but experimental realizable model (accounting detection losses), where changing the value of a parameter of the models changes

*nigam.samantaray@strath.ac.uk

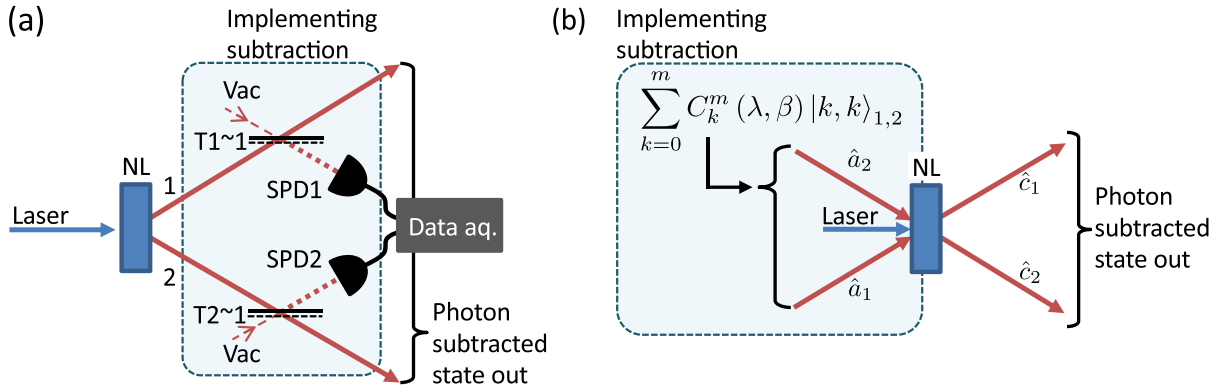

FIG. 1. Equivalent ways of getting a photon subtracted state: (a) the left-hand side image represents the conventional approach in which two high transmittance beam splitters are placed in each path of TBS and a simultaneous photon clicks on the single photon detectors, which confirms the implementation of symmetrical photon subtraction; this subtraction operation can be implemented equivalently by seeding a superposition state to the nonlinear crystal (NL) together with the pump beam as shown in the right image (b).

the TBS individual beam photon statistics from thermal to Poissonian.

For a null value of the model parameter, i.e., when the statistics of individual thermal averaged beams are Poissonian (without thermal averaging the value of the parameter is 1), the resulting state becomes correlated Poissonian TBS (CPTBS), keeping the initial TBS nonclassical mode correlation intact. We then incorporated the symmetrical photon subtraction into the model of absorption measurement. For ease of calculation, we replace the conventional approach of obtaining the photon subtraction (placing high transmittance beam splitters on the individual beam paths) by an alternate way of seeding the photon number superposition state to the squeezer as shown in Fig. 1(b), similar to one reported without thermal averaging in [21].

One of the important goals of this article is to answer the following question. To what extent does photon subtraction bring an advantage for absorption measurement compared to TBS at both fixed squeezing and per photon exposure to the absorbing sample and, furthermore, does photon subtraction provide any advantage particularly when the individual TBS mode statistics turns to Poissonian. The physical significance of considering the fixed squeezing comes due to the fact that optical nonlinearity which relates to squeezing in the SPDC process is usually tiny, resulting in the generation of low mean number of photons. Since photon subtraction increases mean photons of the resulting state, at fixed squeezing, it provides an advantage with respect to its unsubtracted counterpart. Therefore, most of the quantum optics and information protocols demonstrate the advantage of photon subtraction at a fixed squeezing parameter [1,23–25]. The relevance of the second approach, which has been considered up to now only for phase measurement [20,21], is to check if photon subtraction could bring any improvement in photon statistics in addition to an increase in the mean number of photons.

This paper is organized in the following way. In Sec. II, we shall briefly describe the absorption measurement and various types of estimators for loss estimation. The importance of photon statistics and nonclassical correlation in measuring these estimators will also be addressed. Section III contains details about modal averaging and a way to incorporate the photon subtraction operation. We shall also present results for different types of absorption estimators up to two photon subtraction and discuss the usefulness of our model. All the values of the model parameter that change the statistics of TBS from thermal to Poissonian and in between have also been considered in the result. We conclude the paper with a summary in Sec. IV.

II. ABSORPTION MEASUREMENT

Absorption is measured by probing the sample with known light intensity and then measuring the light intensity at the detection stage as shown in Fig. 2, where γ is the absorption coefficient, η is the detection efficiency, and $\langle N_1\rangle$ and $\langle N_1'\rangle$ are the mean number of detected photons before and after placing the sample, respectively. A detector is said to be highly lossy if it has very low detection efficiency or vice versa. The losses due to the presence of the sample and the detection losses are modeled by using a single beam splitter with effective transmittance $\eta\tau$ so that $\langle N_1'\rangle = \tau\langle N_1\rangle$, where $\tau = 1-\gamma$. For applications where low light illumination is required, the uncertainty in measuring γ is dominated by photon shot noise (SN). The uncertainty in absorption measurement due to photon shot noise can be improved by considering two balanced beams($\langle N_1\rangle = \langle N_2\rangle$), which are correlated in the photon number basis as in TBS states generated by the SPDC process. The first beam passes though the sample, whereas the second beam acts as a reference, thus partially canceling the SN going below the shot-noise limit in realistic scenarios. We shall consider three different absorption estimators, namely number difference and optimized balanced [13] including one based on ratio measurement [26], the TBS state as input source, and balanced detection (quantum efficiency η remains the same for both beams) throughout this paper. The estimators considered in this work are not all unbiased. However, we have calculated the uncertainty in measuring the absorption coefficient by propagating uncertainties of associated variables in the estimators. As long as these variables have the same functional form, the associated uncertainties in measuring absorption coefficients remain the same irrespective of whether the estimators are biased or not.

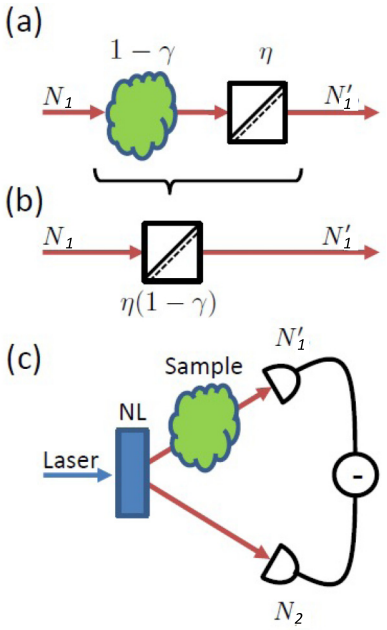

FIG. 2. Absorption measurement: (a) direct one path imaging of a sample object of absorption coefficient γ and η is the detection efficiency, (b) beam splitter equivalence of reflection and detection losses in direct one path imaging, and (c) photon number difference measurement in the presence of quantum correlation generated by pumping the nonlinear crystal in the SPDC process.

The results reported in the article [13] using TBS refer only to a particular experimental situation where a very large number of collected thermal modes each with very low mean photons are averaged and does not show any way of changing their statistics from thermal to Poissonian or vice versa. The principal points of this work are to show the dependence of uncertainties in measuring different absorption estimators on parameters that characterize photon statistics and correlation of the input probe states such as Fano factor (F), and noise reduction factor denoted by the symbol σ, and finding the best absorption measurement for loss estimations in a more general perspective, including photon subtraction. Fano factor is defined as the variance of photon number of a state normalized to its mean value. In terms of statistics, it represents how a state is different from a coherent state. $F > 1$, $F = 1$, and $F < 1$ refers to super-Poissonian, Poissonian, and sub-Poissonian statistics of the light state, respectively. Other related parameters such as second-order autocorrelation function $g^{(2)}(0) = \frac{F-1}{\langle N_1\rangle} + 1$ and Mandel's parameter $Q = F - 1$ can also be useful in place of F. Analogously, for any bipartite state, σ is defined as variance of the photon number difference normalized to their mean. One can easily check $\sigma < 1$ refers to nonclassical photon number correlation. It is worth checking the change in these two parameters when individual TBS mode statistics change from thermal (super-Poissonian) to Poissonian. We have devised a phenomenological model in this context and we shall detail it in the next sections. Furthermore, it is interesting for both fundamental perspectives and applications to see the effect of symmetrica photon subtraction on TBS when its individual beam photon statistics is varied from thermal to Poissonian and to investigate up to what extent the photon subtraction operation is advantageous in this scheme.

A. Number difference measurement

In this measurement, the observable under consideration $\hat{o}(\gamma) = N_2 - N_1'$ is the photon number difference of two beams after placing the object as shown in Fig. 2(c). N_1' and N_2 are the variables which carry photon number fluctuations. Since $\langle\hat{o}\rangle = \gamma\langle N_1\rangle \neq \gamma$, the observable is not an unbiased estimator. As per theory of error propagation, the uncertainty in measuring γ [13,27] is

$$\Delta\gamma_{\text{diff}} = \frac{\sqrt{\Delta^2\hat{o}}}{\left|\frac{\partial\langle\hat{o}\rangle}{\partial\gamma}\right|} = \sqrt{\frac{\gamma^2[F-1] + \gamma + 2\sigma(1-\gamma)}{\langle N_1\rangle}}, \quad (1)$$

where $\langle N_1\rangle = M\eta\,\sinh^2 r = \eta\lambda$ is the total detected mean number of photons of the probe TBS state, r being the squeezing parameter which carries necessary information about the pump intensity and phase-matching function of the SPDC process. M is the total number of modes and it is related to the model parameter as we shall see in the next section. It is easy to check for classical states, i.e, $F = 1$ and $\sigma = 1$, a limit $\Delta\gamma_{\text{diff}} = \sqrt{(2-\gamma)/\langle N_1\rangle}$ known as the shot-noise limit (SNL) in differential absorption measurement. It is paramount to note that, for no absorption ($\gamma = 0$), this limit is twice the standard shot-noise limit in direct one path imaging $1/\sqrt{\langle N_1\rangle}$. Each beam carries one unit of shot noise although, for $\gamma = 1$, standard SNL is reached. It can be checked that, for low values of absorption, i.e., $\gamma \ll 1$, $F = 1$ and $\sigma < 1/2$ allows beating SNL, whereas for relatively high γ, the probe state with $\sigma < 1/2$ and $F < 1$ is required for reaching the SSN limit.

B. Optimized balanced absorption estimator

In the past couple of years, a different absorption estimator of the following form [10] has been considered:

$$\hat{\gamma}_{\text{opt}} = 1 - \frac{N_1' - k\Delta N_2 + \delta E}{\langle N_1\rangle}, \quad (2)$$

where k is a factor to be experimentally determined in order to minimize the uncertainty and δE is a correction factor for making the estimator unbiased so that $\langle\hat{\gamma}_{\text{opt}}\rangle = \gamma$. Exploiting theory of error propagation, uncertainty of this estimator takes the following form [13]:

$$\Delta\gamma_{\text{opt}} = \sqrt{\frac{\gamma(1-\gamma)}{\langle N_1\rangle} + \frac{(1-\gamma)^2\sigma}{\langle N_1\rangle}\left(2 - \frac{\sigma}{F}\right)}. \quad (3)$$

A clear advantage of this estimator is seen as it is $\sqrt{2}$ times advantageous compared to the number difference at low absorption ($\gamma \to 0$) for $\sigma = 1$ and $F = 1$. Another interesting point about this estimator is the requirement of lower quantum correlation, i.e., $\sigma < 1$ ($\sigma < 1/2$ for the number difference case) and $F < 1$ for reaching the SSN limit in the absorption measurement. It can be easily checked for both $\sigma = 0, F = 1$ (perfect photon number correlation and Poissonian individual statistics) and $\sigma = 1, F = 1/2$ (classical photon number correlation and sub-Poissonian individual statistics), the uncertainty in Eq. (3) simplifies to an ultimate quantum limit

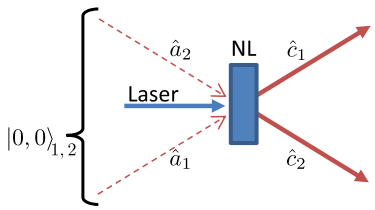

FIG. 3. Scheme for generating correlated TBS states: coherent beam pumps a nonlinear crystal (NL) for generating correlated twin photon states at the exit face of the crystal.

(UQL) [13],

$$\Delta\gamma_{\text{opt}} = \sqrt{\frac{\gamma(1-\gamma)}{\langle N_1\rangle}}. \tag{4}$$

The single mode squeezed vacuum state also reaches this limit for a low mean number of photon $\langle N_1\rangle \to 0$ [28].

C. Ratio measurement

We have considered an estimator based on ratio measurement proposed in the article in [26]. In this measurement the observable we consider is $\hat{o}(\gamma) = N_1'/N_2$ or $\hat{o}(\gamma) = N_2/N_1'$. As $\langle\hat{o}\rangle \neq \gamma$, the estimator is not unbiased. Propagating the uncertainties in N_1' and N_2, we obtain the expression of uncertainty in ratio measurement as

$$\Delta\gamma_{\text{ratio}} = \sqrt{\frac{\gamma(1-\gamma)}{\langle N_1\rangle} + \frac{(1-\gamma)^2 2\sigma}{\langle N_1\rangle}}. \tag{5}$$

Unlike the other two estimators, it shows dependence of the measured absorption uncertainty only on correlation of the probe state σ. It can be checked for $\sigma = 1/2$ and $\sigma = 0$ (perfect quantum correlation) that the corresponding uncertainty becomes SNL (direct one path imaging) and UQL [Eq. (4)], respectively. Thus, similar to the number difference measurement, the ratio estimator beats direct one path imaging when less than 50% of the photon number correlation is lost.

III. MODEL FOR CORRELATED TWB STATE AND SYMMETRICAL PHOTON SUBTRACTION

Let us consider a single correlated photon pair each with mean number of photons λ' generated in the coherence time of the SPDC process as shown in Fig. 3. The mode operators before and after the nonlinear crystal can be easily written as

$$\hat{c_1}(\lambda') = \hat{a_1}\sqrt{1+\lambda'} + \hat{a_2^\dagger}\sqrt{\lambda'}, \tag{6}$$

$$\hat{c_2}(\lambda') = \hat{a_2}\sqrt{1+\lambda} + \hat{a_1^\dagger}\sqrt{\lambda'}. \tag{7}$$

When M numbers of single modes are collected from correlated photon pairs by detectors in a given acquisition time of an experiment, the total average number of collected photons becomes $\lambda = M\lambda'$. Letting $\beta = 1/M$, the input output mode operators can be rewritten in terms of λ as

$$\hat{c_1}(\lambda) \approx \hat{a_1}\sqrt{1+\beta\lambda} + \hat{a_2^\dagger}\sqrt{\beta\lambda}, \tag{8}$$

$$\hat{c_2}(\lambda) \approx \hat{a_2}\sqrt{1+\beta\lambda} + \hat{a_1^\dagger}\sqrt{\beta\lambda}. \tag{9}$$

Both Eqs. (6), (7) and Eqs. (8), (9) are the same and the evolved individual modes follow commutation relation, i.e., $[\hat{c1}, \hat{c1}^\dagger] = \hat{I}$ and $[\hat{c2}, \hat{c2}^\dagger] = \hat{I}$, but the latter provides information about how many individual modes are considered for statistical averaging in order to get the total mean number of photons λ. For the single mode and no averaging case $\lambda' = \beta\lambda$, these sets of equations look like the usual Bougolibov transformation when a vacuum state turns to a two mode squeezed state by an action of a two mode squeezed operator $\hat{S}_{1,2}(\beta\lambda = \lambda')$, whose photon statistics follow:

$$\begin{aligned}
\langle N_1\rangle' &= \langle N_2\rangle' = \beta\eta\lambda,\\
\langle\Delta^2 N_1\rangle' &= \langle\Delta^2 N_2\rangle' = \beta\eta\lambda + \beta^2\eta^2\lambda^2,\\
\langle\Delta(N_1,N_2)\rangle' &= \eta^2(\beta\lambda + \beta^2\lambda^2),\\
\sigma' &= \frac{\langle\Delta^2(N_1-N_2)\rangle}{\langle N_1\rangle + \langle N_2\rangle} = 1-\eta,
\end{aligned} \tag{10}$$

where $\langle N\rangle'$ is the detected mean numbers of photons per mode, the subscripts (1) and (2) correspond to probe (signal) and reference (idler), respectively, and $\langle\Delta^2 N\rangle' = \langle N^2\rangle' - \langle N\rangle'^2$ and $\langle\Delta(N_1,N_2)\rangle' = \langle N_1N_2\rangle' - \langle N_1\rangle'\langle N_2\rangle'$ are the respective variance and covariance. In the experimental situation, the significance of β can be seen as follows: for a single temporal mode in the time window of picoseconds, which is the coherence time τ_{coh} of the SPDC, $\beta = 1$, whereas for more time exposure, many temporal modes are collected and in that case $\beta \approx 0$. The last case is realized for a high temporal band width pump beam so that many more modes $M = \tau_p/\tau_{\text{coh}}$ are generated. This situation is usually considered experimentally for alleviating the excess noise from the individual TBS, demonstrating its usefulness for the SSN absorption measurement [29]. In the past years, a similar situation of the CW pump has been considered, demonstrating experimentally the SSN advantage in reconstructing the absorption profile of an object [10], and more recently in the construction of the SSN raster scanning microscope [11]. Another important point is the effect of pump photon statistics on the generated twin photon statistics via SPDC. Intuitively, $0 \leqslant \beta \leqslant 1$ accounts for all of the last considered experimental situations. Therefore, it is intriguing to consider the parameter β in this model. Detected multimode photon statistics and correlation can be obtained by adding contribution from M numbers of individual modes or equivalently deviding Eq. (10) by the parameter β as follows:

$$\begin{aligned}
\langle N_1\rangle &= \langle N_2\rangle = \eta\lambda,\\
\langle\Delta^2 N_1\rangle &= \langle\Delta^2 N_2\rangle = \eta\lambda + \beta\eta^2\lambda^2,\\
\langle\Delta(N_1,N_2)\rangle &= \eta^2\left(\lambda + \beta\lambda^2\right),\\
\sigma &= \frac{\langle\Delta^2(N_1-N_2)\rangle}{\langle N_1\rangle + \langle N_2\rangle} = 1-\eta = \sigma'.
\end{aligned} \tag{11}$$

An important remark here is that, for balanced detection efficiency, i.e., $\eta_1 = \eta_2 = \eta$, averaged σ is independent of β and is equal to the noise reduction factor of a single correlated mode σ' as it is only limited by η. It implies the photon number correlation remain intact regardless of the values of β. Looking at the expression of variance, when $\beta = 0$, $\langle\Delta N_j^2\rangle = \langle N_j\rangle$ $(j = 1, 2)$, i.e., the individual beam noise has Poissonian

statistics, whereas, for $\beta = 1$, it is easy to see the noise of the individual beam has dominant thermal noise contribution [30], and in this case both Eq. (11) and Eq. (10) give the same result. In a realistic experimental situation, individual modes of the beam remain thermal; it is the averaging over many collected thermal modes that leads to the measurement of Poissonian statistics. Thus the model shows a way to switch from thermal to Poissonian statistics by varying the model parameter β from one to zero.

A. Symmetrical photon subtraction

In this section, we shall see how to incorporate symmetrical photon subtraction taking into account the modal averaging parameter β ($\beta = 1$ case has been theoretically studied up to now [21]).

Theoretically photon subtraction is a nonunitary operation, so a normalization factor is required for getting a symmetrical photon subtracted squeezed vacuum state (thermal single mode case)

$$|\Psi\rangle_m = N_m^-(\beta\lambda)(\hat{a_1})^m(\hat{a_2})^m \hat{S_{1,2}}(\beta\lambda)|0,0\rangle_{1,2}, \tag{12}$$

where N_m^- is the normalization constant of the form

$$N_m^-(\beta\lambda) = m!(-i\sqrt{\beta\lambda})^m P_m(i\sqrt{\beta\lambda}), \tag{13}$$

with P_m being the mth order Legendre's polynomial and m being the number of subtracted photons. In an experimental scenario, two high transmittance beam splitters are placed in the paths of the two beams of the TWB. Two simultaneous clicks at the single photon detectors (SPDS) confirms the probabilistic generation of subtracted states as shown in the left image of Fig. 1. Alternatively by injecting the $m+1$ component superposition state to the NL (squeezer) in place of vacuum equivalently executes deterministically the m photon subtraction operation as shown in Fig. 1(b). Thus the symmetrical photon subtracted state can be equivalently written as

$$\begin{aligned} |\Psi\rangle_m &= \hat{S}_{1,2}(\beta\lambda)|\Phi^s(\beta\lambda)\rangle_m, \\ |\Phi^s(\beta\lambda)\rangle_m &= \sum_{k=0}^{m} C_k^m(\lambda,\beta)|k,k\rangle_{1,2}, \end{aligned} \tag{14}$$

and

$$\begin{aligned} C_k^m(\lambda,\beta) = &\sqrt{\frac{(1+\beta\lambda)^m}{P_m(2\beta\lambda+1)}} \\ &\times \binom{m}{k}\left(\sqrt{\frac{\beta\lambda}{\beta\lambda+1}}\right)^k, \end{aligned} \tag{15}$$

with $\sum_k |C_k^m(\lambda,\beta)|^2 = 1$. Such superposition states $|\Phi^s(\beta\lambda)\rangle_m$ can be experimentally generated [31]. Thus single mode photon subtraction is incorporated by these $m+1$ component superposition states and the set of transformation equations defined in Eq. (8) and Eq. (9). The second method up to now has been realized only for single mode $\beta = 1$. Although both methods give the same result, we have considered the second in our model involving more than one mode (general beta) for making calculations easy.

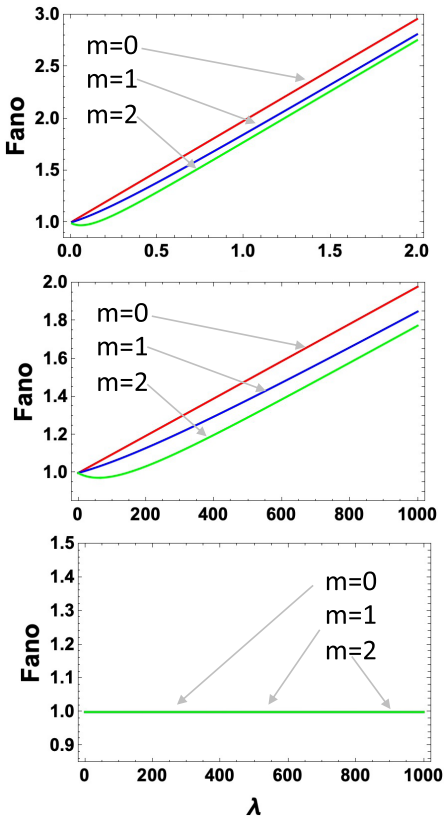

FIG. 4. Plots of Fano factor as a function of λ with $\eta = 0.98$ ($\gamma = 0$) for different values of m: $m = 0$ (solid red line), $m = 1$ (solid blue line), and $m = 2$ (solid green line). We set $\beta = 1$ (top), $\beta = 0.001$ (middle), and $\beta \to 0$ (bottom).

For single mode photon subtracted states, statistics of the transformed operator are obtained by using this input superposition state in place of vacuum. We calculated photon statistics and correlation of the multimode averaged photon subtracted states following the same approach of the squeezed vacuum state discussed earlier in this section. This approach enables calculating photon statistics and correlation of photon subtracted states for a situation involving any value of β. The photon statistics expressions are too cumbersome to present here and we will analyze them graphically. For an experimental point of view, the total collected mean number of photons and modal averaging parameters in connection with the number of modes are important parameters and will be sufficiently discussed throughout the paper. Fano factors of the multimode averaged photon subtracted states are plotted in Fig. 4. It is evident that, for $\beta = 1$ (two individual beams are thermal for $m = 0$), photon subtraction changes the statistics from thermal to sub-Poissonian for low values of the mean number of photons. On the other hand, for $\beta = 0$, when large numbers of modes are averaged (two individual beams are Poissonian as expected), photon subtraction does not provide any further improvement in the statistics. However, for intermediate values of $\beta = 0.001$, i.e., when thousands of modes are averaged, interestingly, the individual beams preserve sub-Poissonian statistics up to a certain range of the total average number of collected photons due to photon subtraction. Moreover, in this case, the states have a higher threshold in terms of λ before

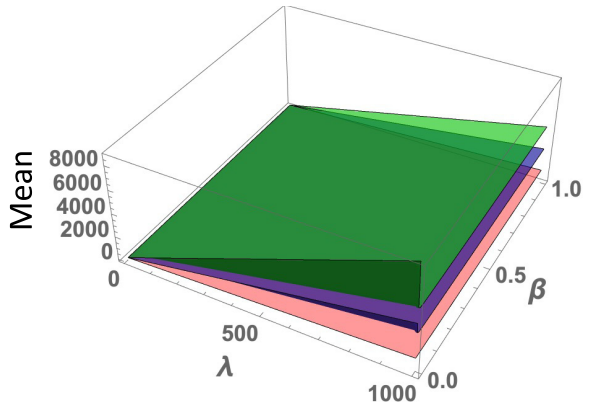

FIG. 5. 3D plots of detected mean number of photons with $\eta = 0.98$ gated by m detections: $m = 0$ (bottom red sheet), $m = 1$ (middle blue sheet), and $m = 2$ (top green sheet).

they become thermal compared to the case of $\beta = 1$. Our calculation shows that the noise reduction factor σ remains the same regardless of the number of photon subtraction m. This is quite expected as, for the balanced case, σ is independent of the statistics of the state and only depends on the detection efficiency.

B. Results

Before interpreting the results, we would like to show the dependence of the mean number of photons per mode with the model parameter β as m changes from 0 to 2. Figure 5 shows the nonlinear rise of the mean number of photons with increasing m. Increase in the mean number of photons is elucidated due to photon subtraction in the TBS and the increment is maximum for $\beta \to 0$ with respect to $\beta = 1$; as in the former case a very large number of modes are involved. Substituting the expression of F and σ in the uncertainty equations for different values of m ($m = 0$–2), we worked out the uncertainties for the above described three absorption estimators. The expressions are too cumbersome to present here, so we shall only depict the results graphically with relevant parameters of interest in the limiting cases.

1. Fixed squeezing parameter

The analysis of comparing uncertainties for different m at fixed squeezing has been carried out at the mean energy (photon number exposure) of the unsubtracted ($m = 0$) state. In this way for a given number of collected modes M, r is fixed as mean energy λ (for $m = 0$)$=M \sinh^2 r$. Uncertainties for number difference measurement is shown in Fig. 6. It shows SSN for different values of m (0–2) in this measurement. Albeit, photon subtraction show the advantage for all values of γ, particularly for low γ and low λ, and $m = 2$ shows maximum advantage of almost three times over $m = 0$ for $\beta = 1$. The magnitude of uncertainty greatly varies with β. For instance, uncertainty improves by a factor of around 100 when 1000 modes are averaged each with $\lambda' = 1$. In this case of $\beta = 0.001$, as λ increases, the thermal noise contribution in terms of F in the uncertainty increases as per Eq. (1), as a result of which the SSN advantage for different m values

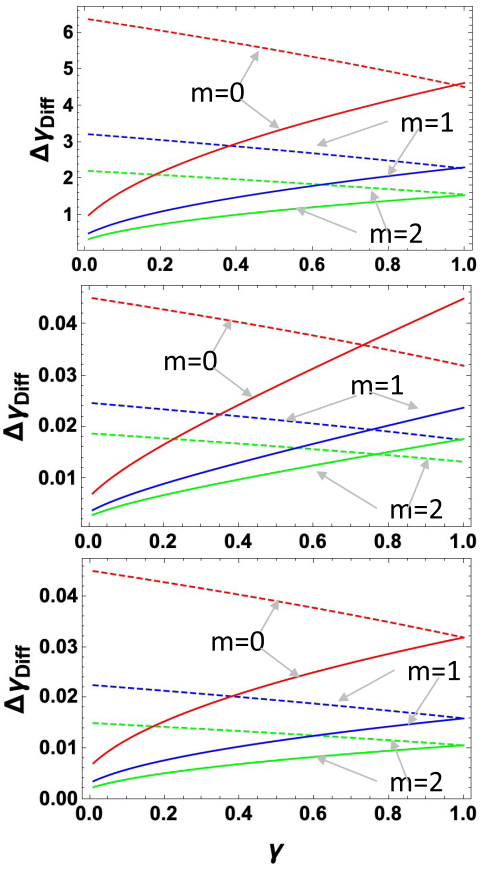

FIG. 6. Plots of uncertainty in the number difference measurement versus absorption coefficient γ with $\eta = 0.98$ for different values of m: $m = 0$ (solid red line), $m = 1$ (solid blue line), and $m = 2$ (solid green line). We set $\lambda = 0.05$, $\beta = 1$ (top), $\lambda = 1000$, $\beta = 0.001$ (middle), and $\lambda = 1000$, $\beta \to 0$ (bottom). Dotted lines are the uncertainties evaluated using classical resources with average energies of the m photon subtracted state.

is lost differently for relative high values of γ, as shown in Fig. 6 (middle). Magnitude of uncertainty remains the same for $\beta \to 0$, i.e., when a very large number of collected modes are averaged to give the same λ as the previously considered $\beta = 0.001$ case. The improvement in uncertainty due to photon subtraction comes only due to an increase in the mean number of photons as the statistics for different m approximates to Poissonian as per Fig. 4 (bottom). In the limit of $\gamma \to 0$ (low absorption) and $\beta \to 0$ (an experimental situation when a large number of modes are usually collected), the uncertainties in the number difference measurement for different m values scale as

$$\Delta\gamma_{\text{diff}}^{m=0} \approx \frac{\sqrt{2(1-\eta)}}{\sqrt{\eta\lambda}},$$
$$\Delta\gamma_{\text{diff}}^{m=1} \approx \frac{\sqrt{(1-\eta)}}{\sqrt{2\eta\lambda}},$$
$$\Delta\gamma_{\text{diff}}^{m=2} \approx \frac{\sqrt{2(1-\eta)}}{3\sqrt{\eta\lambda}}. \tag{16}$$

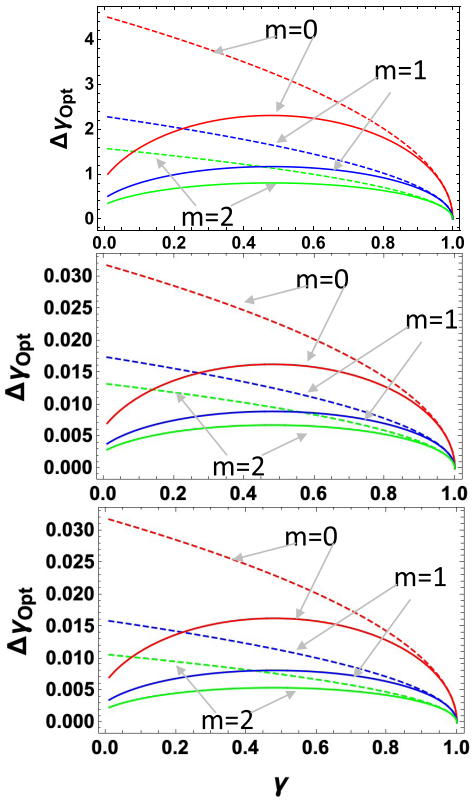

FIG. 7. Plots of uncertainty in the optimized balanced estimator versus absorption coefficient γ with $\eta = 0.98$ for different values of m: $m = 0$ (solid red line), $m = 1$ (solid blue line), and $m = 2$ (solid green line). We set $\lambda = 0.05$, $\beta = 1$ (top), $\lambda = 1000$, $\beta = 0.001$ (middle), and $\lambda = 1000$, $\beta \to 0$ (bottom). Dotted lines are the uncertainties evaluated using classical resources with average energies of the m photon subtracted state.

On the other limiting case of complete absorption ($\gamma \to 1$) and $\beta \to 0$, the uncertainty scales as

$$\Delta\gamma_{\rm diff}^{m=0} \approx \frac{1}{\sqrt{\eta\lambda}},$$
$$\Delta\gamma_{\rm diff}^{m=1} \approx \frac{1}{2\sqrt{\eta\lambda}},$$
$$\Delta\gamma_{\rm diff}^{m=2} \approx \frac{1}{3\sqrt{\eta\lambda}}. \tag{17}$$

This set of equations confirms the standard SNL for the limit $\gamma \to 1$ as per the discussion in Sec. II A. The improvement in the standard SNL for the limit $\gamma \to 0$ comes from a detection efficiency dependent factor $1 - \eta$ in the numerator. The factor of improvements in the same limit due to different number of photon subtraction are also clear.

Normalized uncertainty for the optimized balanced absorption estimator is plotted in Fig. 7. For $\beta = 1$ (thermal case), photon subtraction shows the SSN advantage for all values of γ, particularly for low γ and low λ, and the two photon subtracted state shows maximum advantage of almost three times over TBS without photon subtraction. The magnitude of uncertainty also greatly varies with β. Uncertainty improves by a factor of more than 100 when 1000 modes are averaged each with $\lambda' = 1$. Unlike the number difference estimator, regardless of the values of λ, the uncertainty in the measurement for the optimized balanced absorption estimator is SSN enhanced for $\gamma < 1$. This can be explained from the fact that the contribution of the thermal noise at high λ in the uncertainty of the measurement defined in Eq. (3) of Sec. II B is less significant. Magnitude of uncertainty remains the same for $\beta \to 0$, i.e., when a large number of collected modes are averaged to give the same λ as the $\beta = 0.001$ case. The improvement in uncertainty due to photon subtraction also comes only due to an increase in the mean number of photon as the statistics for different m approximates to Poissonian as per Fig. 4 (bottom). In the limiting case, the uncertainty of the optimized balanced estimator for a different number of subtracted number m can be expressed as follows: for $\gamma \to 0$ (low absorption) and $\beta \to 0$, the uncertainties in the new absorption estimator for different m values scale as

$$\Delta\gamma_{\rm opt}^{m=0} \approx \frac{\sqrt{1-\eta^2}}{\sqrt{\eta\lambda}},$$
$$\Delta\gamma_{\rm opt}^{m=1} \approx \frac{\sqrt{1-\eta^2}}{2\sqrt{\eta\lambda}},$$
$$\Delta\gamma_{\rm opt}^{m=2} \approx \frac{\sqrt{1-\eta^2}}{3\sqrt{\eta\lambda}}. \tag{18}$$

On the other limiting case of complete absorption ($\gamma \to 1$) and for $\beta \to 0$, the uncertainty scales as

$$\Delta\gamma_{\rm opt}^{m=0} \approx \frac{\sqrt{1-\gamma}}{\sqrt{\eta\lambda}},$$
$$\Delta\gamma_{\rm opt}^{m=1} \approx \frac{\sqrt{1-\gamma}}{2\sqrt{\eta\lambda}},$$
$$\Delta\gamma_{\rm opt}^{m=2} \approx \frac{\sqrt{1-\gamma}}{3\sqrt{\eta\lambda}}. \tag{19}$$

Uncertainty given by this set of equations for $\gamma \to 1$ scales much better than the standard SNL and it improves further with the number of subtracted photon m. On the other side of the limit $\gamma \to 0$, apart from a factor $\sqrt{2}$, the improvement in the SNL compared to the number difference measurement comes from a factor $1 - \eta^2$ instead of $1 - \eta$. Also, in this case, there are factors of improvement due to photon subtraction, i.e., $m + 1$ times improvement in m photon subtraction.

A plot of uncertainty in the ratio measurement is shown in Fig. 8. It shows the SSN limit for any values of mean number of photons λ as the uncertainty is unaffected by the thermal noise contribution and only relies on the photon number nonclassical correlation as evident from Eq. (5). Photon subtraction further improves the measurement uncertainty due to increase in the mean photons for thermal case $\beta = 1$. We witnessed a factor of improvement in the magnitude of uncertainty similar to the other two estimators for $\beta = 0.001$. Again, for fixed $\lambda = 1000$, we found the uncertainty for subtracted states ($m = 0$–2) does not change at all as β changes from 0.001 to 0 due to no dependence on photon statistics. Another notable thing is the uncertainty reduction reaching the SSN limit is maximum for low values of γ, which is similar to the case for all our considered absorption estimators. We

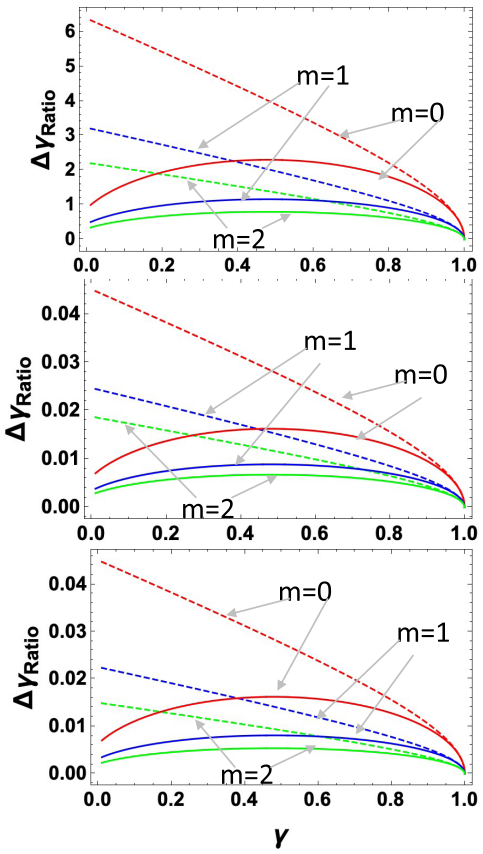

FIG. 8. Plots of uncertainty in the ratio measurement versus absorption coefficient γ with $\eta = 0.98$ for different values of m: $m = 0$ (solid red line), $m = 1$ (solid blue line), and $m = 2$ (solid green line). We set $\lambda = 0.05$, $\beta = 1$ (top), $\lambda = 1000$, $\beta = 0.001$ (middle), and $\lambda = 1000$, $\beta \to 0$ (bottom). Dotted lines are the uncertainties evaluated using classical resources with average energies of the m photon subtracted state.

checked that the uncertainty of the ratio measurement in the limiting case for different numbers of subtracted photons m resembles the uncertainty of the optimized balanced estimator for $\gamma \to 1$ except for $\gamma \to 0$, where the uncertainty matches the uncertainty of the number difference measurement.

We have plotted the uncertainties for different estimators (in a realistic situation where at least 1000 collected modes each with one mean number of photons $\lambda' = 1$ are averaged) showing a comparison among them in Fig. 9. The optimized estimator outperforms the number difference for the full range of absorption. Regardless of the values of γ, the optimized estimator and ratio performs equally well for low detection losses (high detection efficiency η). Nevertheless, in the limit of low γ and at low detection efficiency $\eta = 0.7$, the optimized estimator performs better than the ratio measurement because of the detection efficiency dependent factor $\sqrt{1-\eta^2}$ instead of $\sqrt{1-\eta}$ as per Eq. (18). Photon subtraction shows improvement of nearly more than three times compared to the case of previously considered $\eta = 0.98$ (2% of detection loss) in all these three estimators. Furthermore, the overall magnitude of the uncertainty reduction for these three estimators decreases at this high detection efficiency as they vary

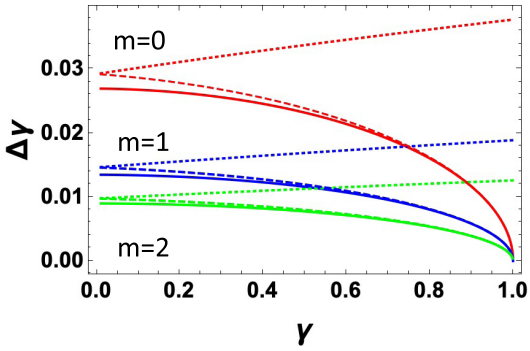

FIG. 9. Comparison of uncertainties among absorption estimators: number difference (dotted), ratio (dashed), and optimized balanced (solid) versus γ for $\eta = 0.7$, $\beta = 0.001$, and $\lambda = 1000$. Different colors correspond to different numbers of photon subtraction.

inversely with η, as evident from the uncertainty equations at their asymptotic limits.

2. *Fixed per photon exposure*

In the meteorological perspective if energy increment is the only consequence of photon subtraction, then it can be easily

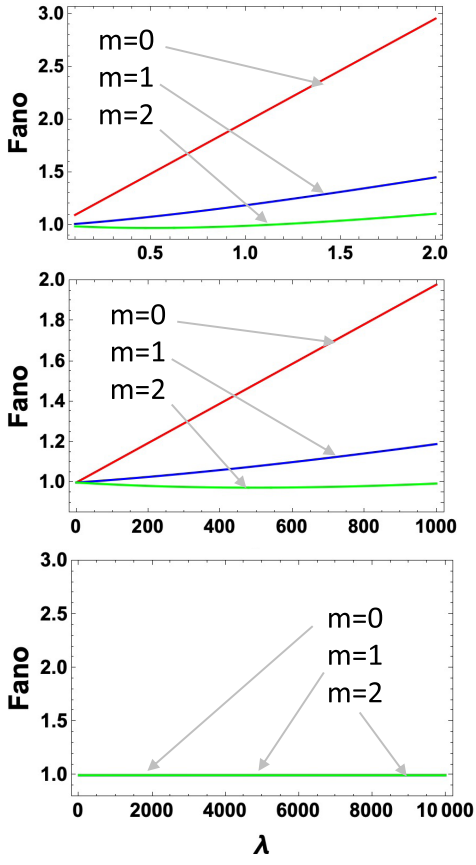

FIG. 10. Plots of Fano factor as a function of λ with $\eta = 0.98$ (and $\gamma = 0$) for different values of m: $m = 0$ (solid red line), $m = 1$ (solid blue line), and $m = 2$ (solid green line). We set $\beta = 1$ (top), $\beta = 0.001$ (middle), and $\beta \to 0$ (bottom).

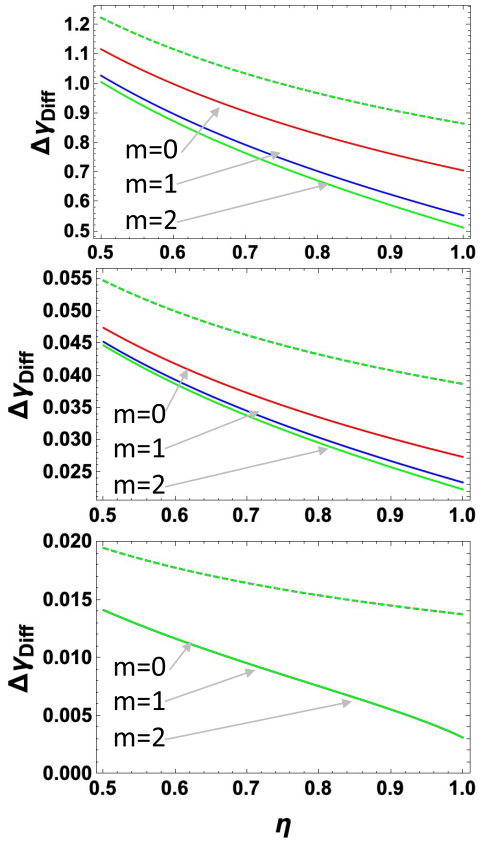

FIG. 11. Plots of uncertainty in the number difference estimator versus efficiency at fixed per photon exposure with $\gamma = 0.5$ for different values of m: $m = 0$ (solid red line), $m = 1$ (solid blue line), and $m = 2$ (solid green line). We set $\beta = 1, \lambda = 2$ (top), $\beta = 0.001, \lambda = 1000$ (middle), and $\beta \to 0, \lambda = 10\,000$ (bottom). Dotted lines are the SNL.

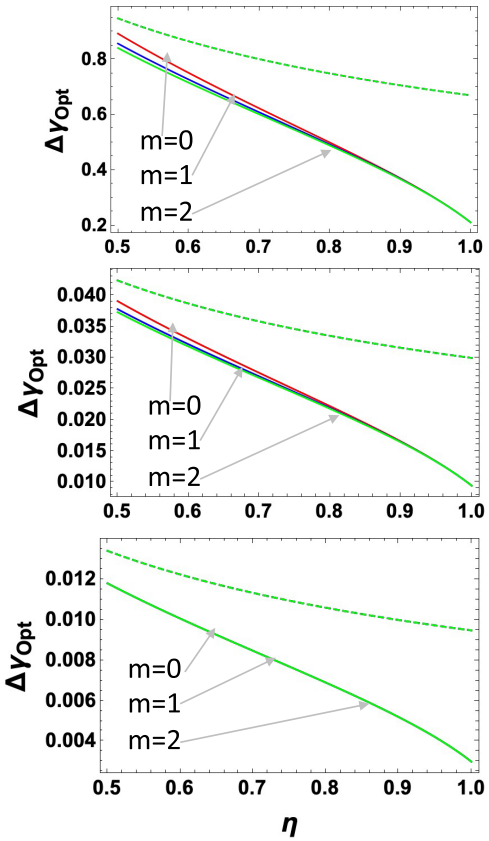

FIG. 12. Plots of uncertainty in the optimized balanced estimator versus detection efficiency in fixed per photon exposure with $\gamma = 0.01$ for different values of m: $m = 0$ (solid red line), $m = 1$ (solid blue line), and $m = 2$ (solid green line). We set $\beta = 1, \lambda = 2$ (top), $\beta = 0.001, \lambda = 1000$ (middle), and $\beta \to 0, \lambda = 10\,000$ (bottom). Dotted lines are the SNL.

accomplished by increasing pump power in the SPDC process. Photon subtraction not only increases the mean energy, but it also improves individual photon statistics. This is why we use the second method to compare equal incident photon flux before and after subtraction. It is paramount to investigate whether or not harnessing photon subtraction could bring any improvement in photon statistics and correlation over classical resources for a situation of general β which can be useful for meteorological applications. In the following, we explore this possibility in detail. Fixed per photon exposure analysis has been carried out by balancing numerically the mean energies of subtracted states so that mean energies for different m are equal to the energy of the $(m = 0)$ unsubtracted state. Since there is a β dependence on mean energy, we further consider the energy balancing at a fixed model parameter. For completeness and generalization of our model, we include very high values of $\lambda = 10\,000$ for $\beta \approx 0$, i.e., when very large number of modes are averaged. Before presenting the uncertainty result, we show the behavior of Fano factor (F) in this energy balancing scenario.

For the $\beta = 1$ (thermal) case, $m = 2$ remaining sub-Poissonian until $\lambda = 1$, while for $m = 1$ and $m = 0$ Fano factor remains super-Poissonian (Fig. 10). Photon subtraction does not provide any advantage for the $\beta = 0$ (Poissonian) case. On the other hand, for $\beta = 0.001$, the sub-Poissonian feature for $m = 2$ preserves up to certain values of λ. This shows a shift in λ to a higher number, and also there is more spacing between different m compared to the case of fixed squeezing.

Uncertainties in the absorption coefficient γ for the number difference measurement is shown in Fig. 11. Unlike the result at fixed squeezing, we checked that the advantage due to photon subtraction is almost lost in the regime of low λ and γ for $\beta = 1$ (thermal). Nevertheless, some advantage still remains at relatively higher λ and γ compared to fixed squeezing. This advantage at relatively high λ can be related to F and, looking at the uncertainty expression in Eq. (1), the advantage at high γ value can be understood from the fact that there must exist a value of γ high enough and detection efficiency sufficiently high to reduce the uncertainty below the SNL. For instance, for values of $\gamma = 0.5$ and $\eta \approx 1$, uncertainty using $m = 0$ is below SNL and $m = 2$ provides almost 20% advantage compared to $m = 0$, although the advantage decreases at low η as evident from Fig. 11 (top). At detection efficiency $\eta = 0.5$, $m = 2$ provides an almost 10% advantage compared to $m = 0$. For $\beta = 0$ (Poissonian), although the magnitude improves due to high $\lambda = 10\,000$, there is no advantage due to photon subtraction as expected. However, for intermediate $\beta = 0.001$, $m = 2$ still outperforms $m = 0$ due to improvement in F.

The magnitude of uncertainty reduction for different m comes closer to $m = 2$ as shown in Fig. 11 (bottom). We expect that as the subtraction parameter m increases the improvements will saturate, converging to a limiting value under which there is no effective gain compared to lower-order photon subtractions. This is clearly visible in the results of Fig. 11, where improvement in measured absorption in fixed (per photon) exposure experiments gets smaller for each increase in m.

Uncertainty for an optimized balanced estimator is plotted in Fig. 12. Like the number difference estimator, the advantage is almost lost for low λ, but still photon subtraction gives a small advantage in the uncertainty reduction for high λ and low γ, and the advantage is more at high detection losses unlike the number difference measurement for $\beta = 1$. For instance, at $\eta = 0.5$, about 10% advantage can be obtained for $m = 2$ compared to $m = 0$. This can be inferred from the uncertainty in Eq. (3), as the uncertainty reduction is more at low detection efficiency η. Though there is an improvement in magnitude, the advantage due to different m is very little and it is not very different compared to $m = 0$ for intermediate $\beta = 0.001$. Similar to the number difference estimator, in this case, the magnitude of the uncertainty reduction for $m = 0, 1$ comes closer to $m = 2$. No improvement is obtained at different m for $\beta = 0$ (Poissonian) for obvious reasons. Since the uncertainty in the ratio estimator in Eq. (5) does not depend on the photon statistics and only depends on photon number correlation, we check that for both $\beta = 1$ and $\beta = 0.001$, unlike the last two estimators, photon subtraction does not provide any advantage in the fixed per photon exposure to the absorption sample including $\beta = 0$ (Poissonian case).

IV. CONCLUSIONS

In summary, we have successfully modeled TBS whose individual beam photon statistics vary between thermal and Poissonian controlled by a "modal averaging parameter" β, and demonstrated their usefulness for loss estimations. We have considered three different ways of measuring the absorption and found the best estimator among them in terms of measured uncertainty reduction accounting for general β, which is relevant for all realistic experimental situations. We established a clear connection between the uncertainty reduction for the three estimators with photon statistics of the individual mode of the TBS and their correlation by two factors, namely Fano factor (F) and noise reduction factor (σ); nonclassicality in these two factors allows sub-shot-noise loss estimations. Furthermore, uncertainties from using the number difference and optimized balanced estimator depends on Fano factor and σ, while, in the ratio measurement, it only depends on the mode correlation σ.

We have then incorporated photon subtraction operation into the model which increases the mean number of photons, and brings further improvement in photon statistics for certain values of the modal averaging parameter β. Correlation remains the same and independent of β, whereas F changes from super-Poissonian to Poissonian when β is varied from one to zero. Photon subtraction improves statistics from super-Poissonian to sub-Poissonian for a single collected mode which further improves with the number of subtracted photons m. In contrast to when a very large number of modes are collected, i.e., for $\beta \to 0$, photon statistics turns to Poissonian and no further improvement is obtained due to photon subtraction. Nevertheless, we have demonstrated for an intermediate value of $\beta = 0.001$ that the sub-Poissonian statistics is preserved up to certain λ.

All the improvements in photon statistics in terms of Fano factor are reflected in the measured uncertainties of the respective estimators. We have analyzed them with respect to different numbers of subtracted photons m by fixing both squeezing parameter and per photon exposure. The last case balances the increased mean number of photons due to photon subtraction. At fixed squeezing, uncertainties in all three absorption estimators scale SSN and maximum uncertainty reduction advantage of three times is obtained for $m = 2$ with respect to $m = 0$ for $\beta = 1$ (thermal case) at very low absorption. The optimized balanced and ratio estimator outperform the number difference estimator. Although the ratio and optimized balanced estimators perform equally well at high detection efficiency, at lower η the latter estimator is slightly better compared to the former. We notice changes in the magnitude of uncertainties with λ and also when more collected modes are averaged. Furthermore, we have explicitly computed the uncertainties at the asymptotic absorption limits ($\gamma = 0, 1$), which confirm all the discussed quantum enhancements in loss estimations due to photon subtraction and show the best absorption estimator as well.

For $\beta = 1$, in the per photon exposure analysis, i.e., when the average photons for different m are held fixed before entering the sample, the advantage due to photon subtraction almost subsides in the low γ and low λ. Nevertheless, for relatively high λ, some advantage of about 20% is preserved for the number difference at high detection efficiency $\eta \approx 1$, and nearly 10% advantage is retained for the optimized balanced estimator at $\eta = 0.5$. Ratio measurement does not give any advantage in the context of photon subtraction at per photon exposure. Photon subtraction retains the advantage for intermediate values of β. Another important remark is that, when very large numbers of modes are averaged, performance of photon subtraction is lost in comparison to unsubtracted states as all of their photon statistics turn to Poissonian in such a scenario. Therefore, photon subtraction in a twin-beam state is advantageous for loss estimation with the single mode thermal case and also when some thermal modes are averaged, but it brings no advantage when very large numbers of modes are averaged, resulting in Poissonian photon statistics.

This work assumes balanced detection efficiency in two beams of the TBS; however, for the unbalancing scenario, the improvement in correlation and statistics may vary and finding the best estimator becomes a potentially challenging task that we will address in future work.

ACKNOWLEDGMENTS

The authors acknowledge support from EPSRC through the QUANTIC Hub EP/T00097X/1, EPSRC early career fellowship EP/M024385/1, and a European Research Council starting grant No. ERC-2018-STG 803665.

[1] S. Olivares, M. G. A. Paris, and R. Bonifacio, Teleportation improvement by inconclusive photon subtraction, Phys. Rev. A **67**, 032314 (2003).

[2] G. Adesso, F. Dell'Anno, S. De Siena, F. Illuminati, and L. A. M. Souza, Optimal estimation of losses at the ultimate quantum limit with non-Gaussian states, Phys. Rev. A **79**, 040305(R) (2009).

[3] M. S. Kim, Recent developments in photon-level operations on travelling light fields, J. Phys. B: At., Mol., Opt. Phys. **41**, 133001 (2008).

[4] V. Parigi, A. Zavatta, M. S. Kim, and M. Bellini, Probing quantum commutation rules by addition and subtraction of single photons to/from a light field, Science **317**, 1890 (2007).

[5] P. R. Tapster, S. F. Seward, and J. G. Rarity, Sub-shot-noise measurement of modulated absorption using parametric down-conversion, Phys. Rev. A **44**, 3266 (1991).

[6] M. V. Chekhova, G. Leuchs, and M. Zukowski, Bright squeezed vacuum: Entanglement of macroscopic light beams, Opt. Commun. **337**, 27 (2015).

[7] G. Brida, L. Caspani, A. Gatti, M. Genovese, A. Meda, and I. R. Berchera, Measurement of Sub-Shot-Noise Spatial Correlations without Background Subtraction, Phys. Rev. Lett. **102**, 213602 (2009).

[8] E. D. Lopaeva, I. R. Berchera, I. P. Degiovanni, S. Olivares, G. Brida, and M. Genovese, Experimental Realization of Quantum Illumination, Phys. Rev. Lett. **110**, 153603 (2013).

[9] N. Samantaray, I. Ruo Berchera, A. Meda, and M. Genovese, Realization of the first sub-shot-noise wide field microscope, Light. Sci. Appl. **6**, e17005 (2017).

[10] P. A. Moreau, J. Sabines-Chesterking, R. Whittaker, S. K. Joshi, P. M. Birchall, A. R. McMillan, J. G. Rarity, and J. C. F. Matthews, Demonstrating an absolute quantum advantage in direct absorption measurement, Sci. Rep. **7**, 6256 (2017).

[11] J. Sabines-Chesterking, A. R. McMillan, P. A. Moreau, S. K. Joshi, S. Knauer, E. Johnston, J. G. Rarity, and J. C. F. Matthews, Twin-beam sub-shot-noise raster-scanning microscope, Opt. Express **27**, 30810 (2019).

[12] J. Sabines-Chesterking, R. Whittaker, S. K. Joshi, P. M. Birchall, P. A. Moreau, A. R. McMillan, H. V. Cable, J. L. O'Brien, J. G. Rarity, and J. C. F. Matthews, Sub-Shot Noise Transmission Measurement Enabled by Active Feed Forward of Heralded Single Photons, Phys. Rev. Appl. **8**, 014016 (2017).

[13] E. Losero, I. R. Berchera, A. Meda, A. Avella, and M. Genovese, Unbiased estimation of an optical loss at the ultimate quantum limit with twin-beams, Sci. Rep. **8**, 7431 (2018).

[14] P. R. Tapster and J. G. Rarity, Photon statistics of pulsed parametric light, J. Mod. Opt. **45**, 595 (1998).

[15] T. S. Iskhakov, V. C. Usenko, R. Filip, M. V. Chekhova, and G. Leuchs, Low-noise macroscopic twin beams, Phys. Rev. A **93**, 043849 (2016).

[16] C. Navarrete-Benlloch, R. Garcia-Patrón, J. H. Shapiro, and N. J. Cerf, Enhancing quantum entanglement by photon addition and subtraction, Phys. Rev. A **86**, 012328 (2012).

[17] T. J. Bartley, P. J. D. Crowley, A. Datta, J. Nunn, L. Zhang, and I. Walmsley, Strategies for enhancing quantum entanglement by local photon subtraction, Phys. Rev. A **87**, 022313 (2013).

[18] A. Ourjoumtsev, A. Dantan, R. Tualle-Brouri, and P. Grangier, Increasing Entanglement between Gaussian States by Coherent Photon Subtraction, Phys. Rev. Lett. **98**, 030502 (2007).

[19] S. L. Zhang, J. S. Guo, W. S. Bao, J. H. Shi, C. H. Jin, X. B. Zou, and G. C. Guo, Quantum illumintion with photon subtracted continuous variable entanglement, Phys. Rev. A **89**, 062309 (2014).

[20] R. Carranza and C. C. Gerry, Photon-subtracted two-mode squeezed vacuum states and applications to quantum-optical interferometry, J. Opt. Soc. Am. B **29**, 2581 (2012).

[21] N. Samantaray, I. Ruo-Berchera, and I. P. Degiovanni, Single phase and correlated phase estimation with multi-photon annihilated squeezed vacuum states, Phys. Rev. A **101**, 063810 (2020).

[22] T. Dirmeier, J. Tiedau, I. Khan, V. Ansari, C. R. Müller, C. Silberhorn, C. Marquardt, and G. Leuchs, Distillation of squeezing using an engineered PDC source, Opt. Express **28**, 30784 (2020).

[23] M. G. Genoni and M. G. A. Paris, Quantifying non-Gaussianity for quantum information, Phys. Rev. A **82**, 052341 (2010).

[24] T. Opatrny, G. Kurizki, and D. G. Welsch, Improvement on teleportation of continuous variables by photon subtraction via conditional measurement, Phys. Rev. A **61**, 032302 (2000).

[25] P. T. Cochrane, T. C. Ralph, and G. J. Milburn, Teleportation improvement by conditional measurements on the two-mode squeezed vacuum, Phys. Rev. A **65**, 062306 (2002).

[26] E. Jakeman and J. G. Rarity, The use of pair production processes to reduce quantum noise in transmission measurements, Opt. Commun. **59**, 219 (1986).

[27] C. C. Gerry and P. L. Knight, *Introductory Quantum Optics* (Cambridge University Press, Cambridge, UK, 2005).

[28] A. Monras and M. G. A. Paris, Optimal Quantum Estimation of Loss in Bosonic Channels, Phys. Rev. Lett. **98**, 160401 (2007).

[29] E. Brambilla, L. Caspani, O. Jedrkiewicz, L. A. Lugiato, and A. Gatti, High-sensitivity imaging with multi-mode twin beams, Phys. Rev. A **77**, 053807 (2008).

[30] A. Meda, E. Losero, N. Samantaray, F. Scafirimuto, S. Pradyumna, A. Avella, I. R. Berchera, and M. Genovese, Photon-number correlation for quantum enhanced imaging and sensing, J. Opt. **19**, 094002 (2017).

[31] S. Lee, J. Park, H. Lee, and H. Nha, Generating arbitrary photon-number entangled states for continuous-variable quantum informatics, Opt. Express **20**, 14221 (2012).